Donor-π-Acceptor Conjugated Copolymers for Photovoltaic Applications: Tuning the Open-Circuit Voltage by Adjusting the Donor/Acceptor Ratio

Qiang Peng,[†] Kuyson Park,[†] Tong Lin,[‡] Michael Durstock,[§] and Liming Dai*[,†,||]

Department of Chemical and Materials Engineering, School of Engineering and Department of Chemistry and UDRI, University of Dayton, 300 College Park, Dayton, Ohio 45469, Centre for Material and Fibre Innovation, Deakin University, Victoria 3217, Australia, and Materials and Manufacturing Directorate, Air Force Research Laboratory, AFRL/MLBP, Wright-Patterson Air Force Base, Dayton, Ohio 45433

Received: August 9, 2007; In Final Form: December 12, 2007

A class of new conjugated copolymers containing a donor (thiophene)−acceptor (2-pyran-4-ylidene-malononitrile) was synthesized via Stille coupling polymerization. The resulting copolymers were characterized by ^{1}H NMR, elemental analysis, GPC, TGA, and DSC. UV−vis spectra indicated that the increase in the content of the thiophene units increased the interaction between the polymer main chains to cause a red-shift in the optical absorbance. Cyclic voltammetry was used to estimate the energy levels of the lowest unoccupied molecular orbital (LUMO) and the highest occupied molecular orbital (HOMO) and the band gap (E_g) of the copolymers. The basic electronic structures of the copolymers were also studied by DFT calculations with the GGA/B3LYP function. Both the experimental and the calculated results indicated an increase in the HOMO energy level with increasing the content of thiophene units, whereas the corresponding change in the LUMO energy level was much smaller. Polymer photovoltaic cells of a bulk heterojunction were fabricated with the structure of ITO/PEDOT/PSS (30 nm)/copolymer−PCBM blend (70 nm)/Ca (8 nm)/Al (140 nm). It was found that the open-circuit voltage (V_{oc}) increased (up to 0.93 V) with a decrease in the content of thiophene units. Although the observed power convention efficiency is still relatively low (up to 0.9%), the corresponding low fill factor (0.29) indicates considerable room for further improvement in the device performance. These results provided a novel concept for developing high V_{oc} photovoltaic cells based on donor-π-acceptor conjugated copolymers by adjusting the donor/acceptor ratio.

1. Introduction

Polymer photovoltaic cells (PVCs) have received considerable attention due to their versatility in the fabrication of lightweight, flexible devices with great promise to provide environmentally friendly, inexpensive, and renewable energy from sunlight.[1−9] One of the promising strategies for devising efficient PVCs involves the use of well-ordered bulk heterojunctions based on a blend of electron-donating conjugated polymers and soluble fullerene acceptors as the photoelectric conversion layer.[2] For instance, bulk heterojunction PVCs made from a blend of regioregular poly(3-hexylthiophene) (P3HT) as the donor and 1-(3-methoxycarbonyl)propyl-1-phenyl-6,6-methanofullerence (PCBM) as the acceptor have recently been shown to yield power conversion efficiencies (PCE) up to 3−5%.[6,7,10−14] The reported high power conversion efficiencies have been attributed to the formation of self-organized P3HT lamellar microstructures that can not only improve the charge-carrier mobility but also extend the optical absorption spectrum to longer wavelengths.[15]

Although the formation of nanosized phase structures is good for improving the power conversion efficiency of organic bulk heterojunction PVCs, phase separation to form domains larger than the exciton diffusion length often leads to a decrease in the power conversion efficiency. Indeed, phase separation between the polymer donor and the fullerene acceptor remains one of the main problems for the conjugated polymer/soluble fullerene-based bulk heterojunction PVCs, especially those with a high fullerene content. As a result of the phase separation, the device lifetime is reduced, the charge separation/transportation within the active layer is suppressed, and hence, there is a reduced device efficiency as well.[16−21] To minimize the donor−acceptor phase separation, conjugated polymers having electron-donating (D) and electron-accepting (A) moieties in the same main chain were investigated.[17−27] Intramolecular charge transfer in these D-π-A polymers reduces the demand for a high content of fullerene and offers a better interfacial contact between the donor and the acceptor, leading to a minimized phase separation. Moreover, physical properties of the donor−acceptor polymers can be easily tuned over a wide range by tailoring structures of the donor and acceptor moieties and/or the linking bridge(s).[28,29] Such a structural optimization could provide an effective means not only for enhancing the carrier mobility and solar absorption but also for increasing the open-circuit voltages (V_{oc}) that are determined by the energy difference between the HOMO level of the electron-donating conjugated polymer and the LUMO level of the electron-accepting fullerene. Thus, the use of a photovoltaic active polymer that has a low HOMO level could be an effective way to achieve high V_{oc} photovoltaic devices.[19] The usually low V_{oc} has recently been recognized as one of the limiting factors leading to low efficiencies for conventional bulk-heterojunction organic photovoltaic cells.[19]

In this study, we used thiophene and 2-pyran-4-ylidene-malononitrile (PYM) as the electron donor and acceptor unit,

* Corresponding author. E-mail: ldai@udayton.edu.
† School of Engineering, University of Dayton.
‡ Deakin University.
§ Wright-Patterson Air Force Base.
|| Department of Chemistry and UDRI, University of Dayton.

10.1021/jp7105428 CCC: $40.75
Published on Web 02/19/2008

SCHEME 1: Synthetic Routes to Monomers and Copolymers

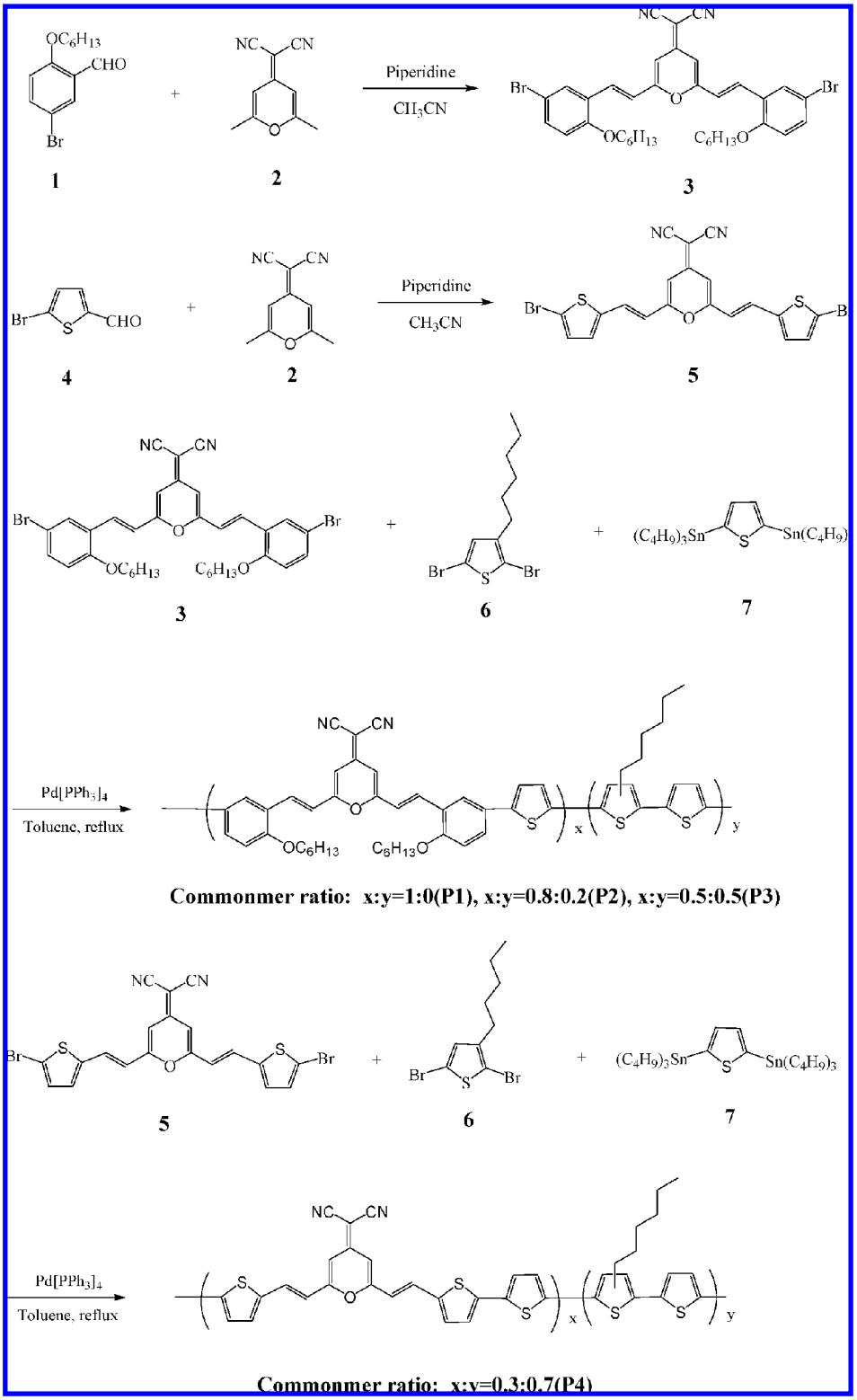

respectively, to synthesize D-π-A conjugated copolymers (Scheme 1). By characterizing the optical absorption, electrochemical, and PV device characteristics of the copolymers having different thiophene/PYM ratios, we found that the band gap energy and the HOMO energy level of the copolymer can be effectively tuned by adjusting the donor/acceptor ratio in the copolymer structure. As a result, the V_{oc} value was found to increase with a decrease in the thiophene content.

Thiophene was chosen as the electron-donating moiety as polythiophene has been shown to have an excellent electron-donating ability and electrochemical stability in PVC devices.[1] Also, cyano is a strong electron-withdrawing group and has been proven to increase electron affinity and to facilitate electron injection.[30] Besides, the use of the phenylene vinylene unit to connect PYM is expected to increase the V_{oc} of the bulk heterojunction PVCs.[31,32]

2. Experimental Procedures

2.1. Materials and Characterization. All chemical reagents were purchased from Fisher Scientific Co. or Aldrich Chemical

Co. and were used as received, unless stated otherwise. All solvents were distilled over appropriate drying agent(s) prior to use and were purged with nitrogen. All manipulations involving air-sensitive reagents were performed in a dry argon atmosphere. ^{1}H NMR spectra were recorded on a Bruker Avance 3000 spectrometer with chloroform-*d* as the solvent and tetramethylsilane as the internal standard. Elemental analyses were conducted by Atlantic Microlab Inc. Cyclic voltammetry (CV) measurements were performed on an eDAQ potentiostat electrochemical analyzer using a three-electrode cell with a platinum plate working electrode, a platinum wire counter electrode, and Ag/AgCl (0.1 mol/L) reference electrode at a scan rate of 50 mV/s. Tetrabutylammonium hexafluorophosphate (Bu_4NPF_6) in an anhydrous and nitrogen-saturated acetonitrile (CH_3CN) solution (0.1 mol/L) was used as the supporting electrolyte. Polymers to be measured were coated on the platinum plate working electrodes from dilute chloroform solutions.

UV−vis and fluorescence spectra were recorded on a PerkinElmer Lambda 900 UV−vis/NIR spectrometer and a PerkinElmer LS 55 spectrometer, respectively. Thermogravimetric analyses (TGA) were conducted on a TA Instruments Model TGA Q500 thermogravimetric analyzer at a heating rate of 10 °C min^{-1} under N_2 flow (90 mL min^{-1}). Differential scanning calorimetry (DSC) measurements were carried out using a TA Instrument Model DSC Q100 system at a heating rate of 10 °C min^{-1} under N_2.

Polymer photovoltaic cells were fabricated using ITO glass as an anode and Ca/Al as a cathode. In a typical experiment, we first solution-spun a PEDOT/PSS aqueous solution (Baytron 4083/Bayer, used as received) to form a thin coating layer with a thickness of 30 nm onto the clean ITO surface. A blend of the as-synthesized copolymer and PCBM (1:1 w/w) was then spin-coated from a chlorobenzene solution (20 mg/mL) onto the ITO/PEDOT/PSS electrode to form the photosensitive layer (∼70 nm). Metal Ca (8 nm) and Al (140 nm) were sequentially deposited onto the photosensitive layer by thermal evaporation under 9×10^{-7} Torr. The effective area of the device was 4 mm^2. The thickness of films was measured using a Dektak 6M surface profilometer. The device current−voltage (*I*−*V*) characteristics were measured with a computer-controlled Keithley 236 Source Measurement system. A solar simulator was used as the light source (AM1.5, 100 mW/cm^2), and the light intensity was monitored by a standard Si solar cell.

The molecular geometry and electronic calculations were made with DFT quantum mechanical code, DMol^3, based on the generalized gradient corrected (GGA) functional B3LYP.[33−35]

2.2. Monomer Syntheses. *2.2.1. 2-{2,6-Bis[2-(2-hexyloxyl-5-bromophenyl)vinyl]pyran-4-ylidene}-malononitrile (3).*[36] A mixture of 2-hexyloxyl-5-bromobenzaldehyde (**1**) (5.70 g, 20.0 mmol), 2-(2,6-dimethylpyran-4-ylidene)malononitrile (**2**) (1.72 g, 10.0 mmol), piperidine (0.2 mL), and freshly distilled acetonitrile (30 mL) was refluxed under argon for 24 h. The reaction mixture was cooled to room temperature. The yellow precipitate was filtered and washed with 50 mL of acetonitrile. The crude product was purified by silica gel column chromatography using chloroform as the eluent. Compound **3** was obtained as a yellow solid with a yield of 72%. ^{1}H NMR ($CDCl_3$, 300 MHz, δ/ppm): 7.74−7.61 (m, 4H), 7.49−7.42 (m, 2H), 6.98−6.67 (m, 6H), 4.09−4.04 (t, 4H), 1.92−0.80 (m, 22H). Anal. calcd for $C_{36}H_{38}Br_2N_2O_3$: C, 61.20; H, 5.42; N, 3.96. Found: C, 61.42; H, 5.59; N, 4.25.

2.2.2. 2-{2,6-Bis[2-(4-bromothienyl)vinyl]pyran-4-ylidene}-malononitrile (5).[37] A mixture of 5-bromo-2-thiophenecarboxaldehyde (**4**) (1.91 g, 10.0 mmol), 2-(2, 6-dimethylpyran-4-ylidene)malononitrile (**2**) (0.86 g, 5.00 mmol), piperidine (10 drops), and freshly distilled acetonitrile (10 mL) were refluxed under argon for 24 h. The reaction mixture was cooled to room temperature. The dark red precipitate was filtered and washed with 50 mL of acetonitrile. The crude product was purified by recrystallization from methanol to afford compound **5** as a dark red solid with a yield of 76%. ^{1}H NMR ($CDCl_3$, 300 MHz, δ/ppm): 7.91−7.86 (d, 2H), 7.38−7.33 (m, 4H), 7.11−6.93 (d, 4H). Anal. calcd for $C_{20}H_{10}N_2S_2OBr_2$: C, 46.36%; H, 1.95%; N, 5.41%; S, 12.35%. Found: C, 46.31%; H, 1.92%; N, 5.49%; S, 12.17%.

2.3. Copolymer Syntheses. In a typical experiment, 1.0 mmol of the compound **3**, 2,5-dibromo-3-hexyl-thiphene (**6**), and 2,5-bis(tributylstannyl)thiophene (**7**) mixture was put into a 100 mL three-necked flask. The feed ratio for each of the components in the mixture was controlled at different values for the preparation of different copolymers (vide infra). To the mixture solution, 20 mL of degassed toluene was added under the protection of argon, followed by flushing the solution with argon for 10 min. A total of 50 mg of $Pd(PPh_3)_4$ and 1.0 mmol of 2,5-bis(tributylstannyl)thiophene were then added into the mixture solution. After another flushing with argon for 20 min, the reactant mixture was heated and refluxed for 24 h. Thereafter, the reaction solution was cooled to room temperature and precipitated by the addition of 200 mL of methanol. The crude copolymer was filtered and extracted in a Soxhlet apparatus with methanol, hexane, and acetone. The copolymer was then obtained as a solid powder and dried under vacuum for 12 h to afford the final product. The yields of the polymerization reactions were about 42−53%.

2.3.1. P1. Compound **3** (0.707 g, 1.0 mmol), 2,5-bis(tributylstannyl)thiophene (**7**) (0.662 g, 1.0 mmol), toluene (20 mL), and $Pd(PPh_3)_4$ (0.05 g, 0.043 mmol) were used, and the general procedure described previously for the copolymer syntheses was followed (cf. Scheme 1). The obtained solid was a dark red powder with a yield of 42%. $M_w = 6500$, $M_w/M_n = 2.12$. ^{1}H NMR ($CDCl_3$, 300 MHz, δ/ppm): 7.63−7.60 (m), 7.40−7.28 (m), 7.06−6.66 (m), 4.10 (s), 1.88−0.78 (m). Anal. calcd for $(C_{40}H_{40}O_3N_2S)_n$ C, 76.41; H, 6.41; N, 4.46. Found: C, 74.37; H, 6.52; N, 4.01.

2.3.2. P2. Compound **3** (0.565 g, 0.8 mmol), 2,5-dibromo-3-hexyl-thiphene (**6**) (0.0652 g, 0.2 mmol), 2,5-bis(tributylstannyl)thiophene (**7**) (0.662 g, 1.0 mmol), toluene (20 mL), and $Pd(PPh_3)_4$ (0.05 g, 0.043 mmol) were used, and the general procedure described previously for the copolymer syntheses was followed (cf. Scheme 1). The obtained solid was a dark red powder with a yield of 48%. $M_w = 5600$, $M_w/M_n = 1.78$. ^{1}H NMR ($CDCl_3$, 300 MHz, δ/ppm): 7.85−7.57 (m), 7.40−7.22 (m), 7.06−6.68 (m), 4.10 (d), 2.76 (s), 1.87−0.79 (m). Anal. calcd for $(C_{35.32}H_{35.68}S_{1.18}O_{2.46}N_{1.64})_n$ C, 75.72; H, 6.42; N, 4.10. Found: C, 74.68; H, 6.49; N, 3.72.

2.3.3. P3. Compound **3** (0.353 g, 0.5 mmol), 2,5-dibromo-3-hexyl-thiphene (**6**) (0.163 g, 0.5 mmol), 2,5-bis(tributylstannyl)thiophene (**7**) (0.662 g, 1.0 mmol), toluene (20 mL), and $Pd(PPh_3)_4$ (0.05 g, 0.043 mmol) were used, and the general procedure described previously for the copolymer syntheses was followed (cf. Scheme 1). The resulting solid was a dark red powder with a yield of 53%. $M_w = 4200$, $M_w/M_n = 1.65$. ^{1}H NMR ($CDCl_3$, 300 MHz, δ/ppm): 7.88−7.51 (m), 7.39−7.21 (m), 7.08−6.65 (m), 4.09 (d), 2.76 (s), 1.87−0.79 (m). Anal. calcd for $(C_{28.04}H_{28.96}S_{1.46}O_{1.5}N_{1.08})_n$ C, 74.54; H, 6.46; N, 3.35. Found: C, 72.64; H, 6.55; N, 2.98.

2.3.4. P4. Compound **5** (0.155 g, 0.3 mmol), 2,5-dibromo-

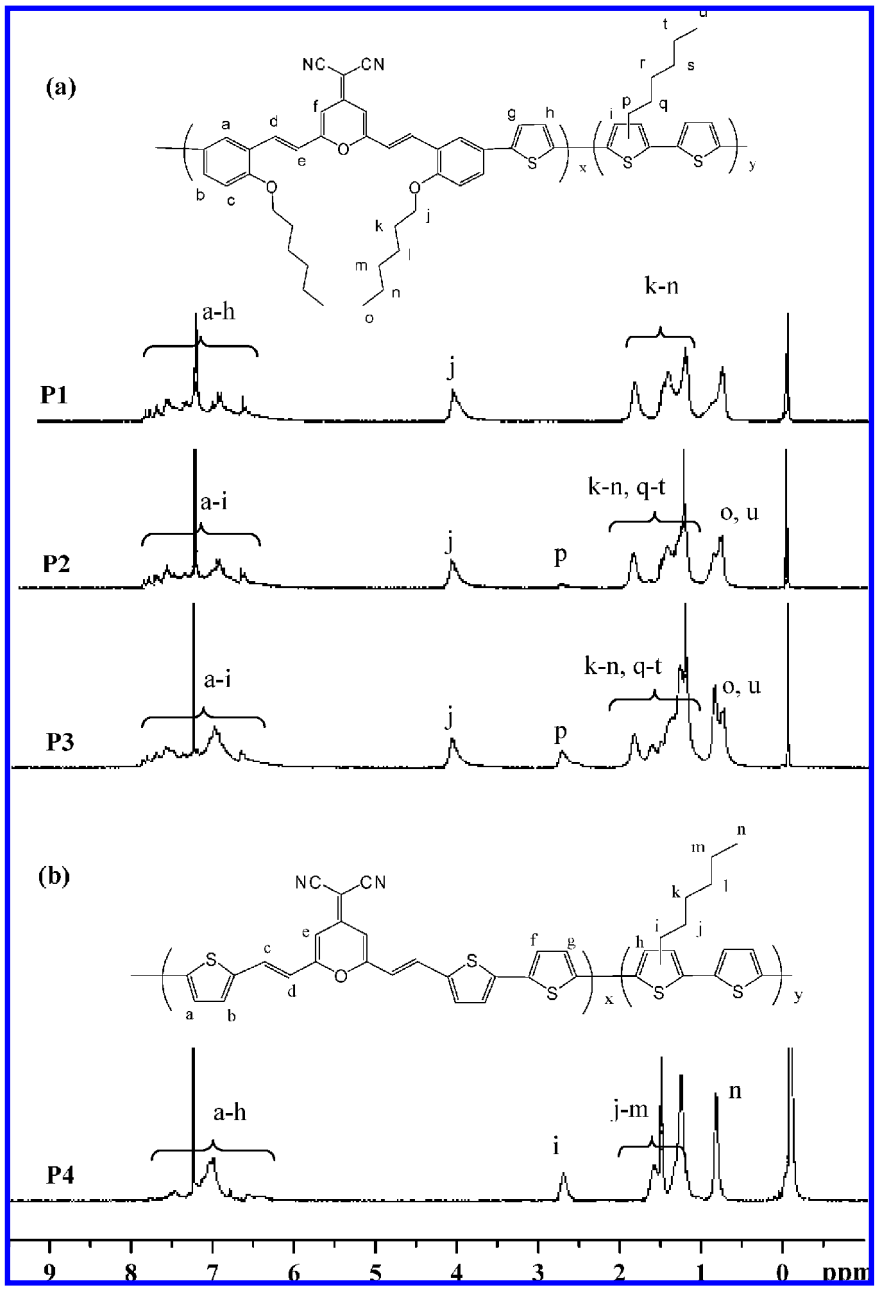

Figure 1. ^{1}H NMR spectra of **P1**−**P4** for determination of the compolymer compositions.

3-hexyl-thiphene (**6**) (0.228 g, 0.7 mmol), 2,5-bis(tributylstannyl)thiophene (**7**) (0.662 g, 1.0 mmol), toluene (20 mL), and $Pd(PPh_3)_4$ (0.05 g, 0.043 mmol) were used, and the general procedure described previously for the copolymer syntheses was followed (cf. Scheme 1). The resulting solid was a dark red powder with a yield of 55%. $M_w = 5300$, $M_w/M_n = 1.72$. ^{1}H NMR ($CDCl_3$, 300 MHz, δ/ppm): 7.80−7.44 (m), 7.33−7.22 (m), 7.16−6.43 (m), 2.76 (s), 1.67−0.89 (m). Anal. calcd for $(C_{16.9}H_{14.84}S_{2.29}O_{0.29}N_{0.58})_n$ C, 66.77; H, 4.92; N, 2.67. Found: C, 66.62; H, 5.03; N, 2.78.

3. Results and Discussion

3.1. Synthesis and Characterization of the Copolymers. Scheme 1 shows the synthetic route to the monomers **3** and **5** and the corresponding copolymers **P1**−**P4**. The monomers **3** and **5** were prepared through Knoevenagel condensation of 2-(2,6-dimethypyran-4-ylidene)malomonitrile (**2**) with 2-hexyloxyl-5-bromobenzaldehyde (**1**) and 5-bromo-2-thiophenecarboxaldehyde (**4**), respectively, at a yield of over 70%.[36,37] Polymerization of the monomer **3** with 2,5-bis(tributylstannyl)-thiophene (**7**) in toluene in the presence of a $Pd[PPh_3]_4$ catalyst yielded the copolymer **P1**, while the reaction of monomers **3** or **5** with **7** and 2,5-dibromo-3-hexyl-thiphene (**6**) at different molar ratios produced the copolymers **P2**−**P4**.

Figure 1 depicts the typical ^{1}H NMR spectra for the copolymers synthesized in this study, in which all the peaks have been assigned to their corresponding protons in each of the macromolecular structures. As can be seen in Scheme 1, polymer **P1** is an alternating copolymer of monomer **3** and 2,5-bis(tributylstannyl)thiophene (**7**), while polymers **P2** and **P3** are random copolymers of **P1** and 5,5′-poly(3-hexyl-2,2′-bithiophene) with different molar ratios of the monomer **3** to 2,5-dibromo-3-hexylthiophene (**6**). While a predetermined molar ratio of compound **3** to 2,5-dibromo-3-hexylthiophene (**6**) was used for each of the experiments, the actual ratio of *x*/*y* for each of the resultant copolymers was determined from proton peaks of the

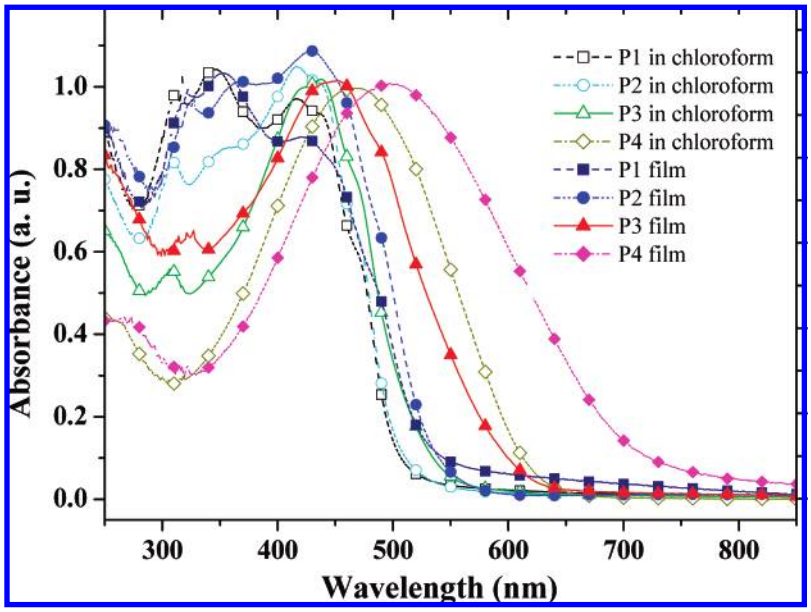

Figure 2. Absorption spectra of **P1**−**P4** in chloroform and in the solid state by spin-coating on quartz plates.

TABLE 1: Polymer Structure, Optical Absorption, and Energy-Level Data

		P1	P2	P3	P4
M_w		6500	5600	4200	5300
x/y		0	0.18/0.82	0.46/0.54	0.29/0.71
$\lambda_{max}^{chloroform}$ (nm)		318, 345, 419	311, 356, 418	310, 422, 438	469
λ_{max}^{film} (nm)		322, 356, 426	325, 367, 430	326, 455	503
E_g (eV)	abs	2.33	2.21	1.99	1.76
	CV	2.20	2.18	2.13	1.81
	DFT	1.84	1.31		1.61
E_{HOMO} (eV)	CV	−5.17	−5.10	−5.01	−4.99
	DFT	−5.10	−4.56		−4.86
E_{LUMO} (eV)	CV	−2.97	−2.92	−2.88	−3.18
	DFT	−3.26	−3.25		−3.25

hexyloxy and hexyl groups shown in the ^{1}H NMR spectra (Figure 1a). For **P1**, the proton peak at $\delta = 4.10$ ppm is attributable to the hydrogen at position j on the hexyloxy side chains attached to the phenyl rings. Apart from the proton peak at $\delta = 4.10$ ppm, both **P2** and **P3** display a new peak at 2.76 ppm associated with the hydrogen at position p on the hexyl side chain of the 3-hexyl-2,2′-bithiophene unit. Therefore, the ratio of x/y for **P2** and **P3** can be estimated from the ratio of the integral areas of peaks j and p to be 0.82:0.18 and 0.54:0.46, respectively, consistent with the monomer feed ratios. On the other hand, a predetermined molar ratio of compound **5** to 2,5-dibromo-3-hexylthiophene (**6**) was also used for the preparation of **P4**. When the feed ratio x/y was over 0.3:0.7, the resulting copolymers became insoluble in organic solvent. As shown in Figure 1b, the peak at 2.76 ppm is due to the hydrogen at position i, while the multi-peaks in the range of 7.80−6.43 are associated with the hydrogen atoms a−h of the thiophene, PYM cycles, and ethylene. From the ratio of the integral areas of the peaks i and a−h, the ratio of x/y for **P4** can be estimated to be 0.29:0.71.

GPC measurements showed that the resultant copolymers possess weight-average molecular weights (M_w) and polydispersity indices (M_w/M_n) in the range of 4100−6500 and 1.65−2.12, respectively. The observed relatively low polymerization degree and broad molecular weight distribution are due to the ineffectiveness of the Stille polycondensation for producing polymers with a high molecular weight. Similar results have been reported for other alternating copolymers prepared by the Stille polycondensation.[38−40] These copolymers can be easily dissolved in common organic solvents for structural characterization and device fabrication, although some care is needed to prepare cohesive and pinhole-free thin films from them. Indeed, the resulting polymers are easily soluble in common organic solvents, such as chloroform, tetrahydrofuran, toluene, xylene, and chlorobenzene, even at room temperature. Uniform and transparent films can be formed by spin-coating the polymer−toluene solution (10 mg/mL) on ITO glasses with a spin rate of 1500 rpm.

The thermal stability of the copolymers was evaluated by TGA under a nitrogen atmosphere. Polymers **P1**−**P4** exhibited good thermal stabilities with decomposition onset temperatures at 278, 266, 262, and 269 °C, respectively. DSC measurements were also performed, and the glass transition temperatures of **P1**−**P4** were determined to be 74, 75, 78, and 76 °C, respectively. These results suggest that the resulting polymers have adequate thermal properties required for the fabrication of PVCs and other optoelectronic devices.

3.2. UV−vis Absorption. UV−vis absorption spectra of the copolymers in dilute chloroform solution (concentration 1×10^{-5} M) are shown in Figure 2, and the maximum absorptions are listed in Table 1. The polymer **P1** shows optical absorption in both the UV and the visible regions with the maximum absorption peaks located at 318, 345, and 419 nm, arising from the $\pi-\pi^*$ transition within the polymer backbone. In comparison to **P1**, copolymers **P2** and **P3** exhibited much weaker absorption in the UV region, due to possible intramolecular charge transfer over a relatively long conjugation length along the copolymer backbones. With the increase in the content of

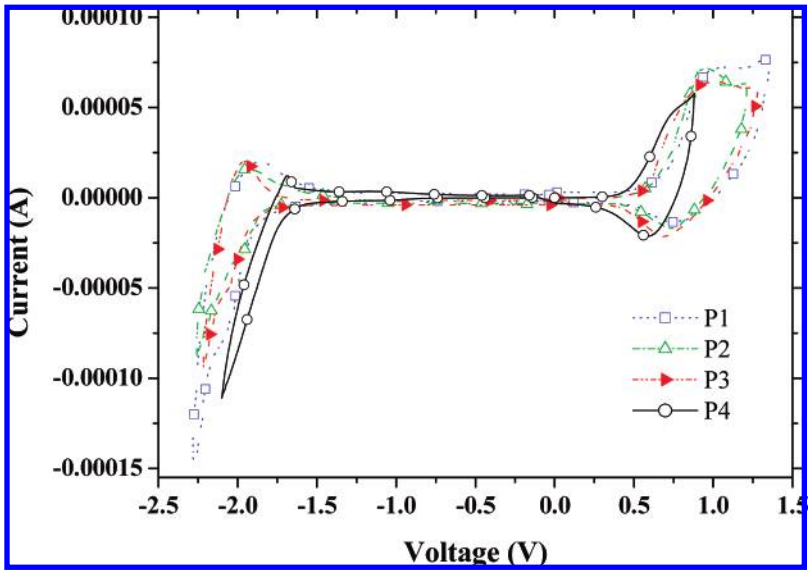

Figure 3. Cyclic voltammograms of **P1**−**P4** recorded from a thin film coated onto platinum plate electrodes in an electrolyte solution of Bu_4NPF_6 (0.10 M) in acetonitrile with a Ag/AgCl (0.10 M) reference electrode recorded at room temperature. Scan rate was 50 mV s^{-1}.

thiophene units from **P1** to **P3**, the visible absorption was further enhanced along with the rapid decrease in their absorption in the UV region, indicating, once again, an increase in the conjugation length. The maximum absorption peak for **P4** was located at 469 nm, indicating that the replacement of a phenyl unit by thiophene efficiently increased the conjugation length.

The optical absorption spectra in the film state were also measured (Figure 2) with their absorption peak intensities listed in Table 1. As compared to their counterparts in the solution state, the polymer films showed a slight red-shift in their optical absorption, presumably indicating the formation of a π-stacked structure in the solid state[41] that could facilitate charge transportation for photovoltaic applications. The energy band gaps calculated from the absorption band edges of the optical absorption spectra were about 2.33, 2.21, 1.99, and 1.76 eV for polymers **P1**−**P4**, respectively, indicating an effective narrowing in the band gap energy by increasing the thiophene content in the polymer backbone.

3.3. Electrochemical Properties. The redox behaviors of the copolymer films were studied by CV. As seen in Figure 3, all the copolymers show a reasonably good reversibility in both the *n*-doping and the *p*-doping processes. On the anodic sweep, the oxidation peaks for **P1**−**P4** were found to be at 1.01, 0.89, 1.05, and 0.88 V, respectively, with the corresponding rereduction peaks at 0.79, 0.59, 0.61, and 0.58 V. The corresponding onset potentials for the *p*-doping processes were determined to be 0.52, 0.45, 0.36, and 0.34 V. In contrast, the cathodic sweep showed reduction peaks at −2.22, −2.20, −2.18, and −2.10 V for **P1**−**P4**, respectively, and the corresponding reoxidation peaks at −1.78, −1.86, −1.92, and −1.69 V. The onset potentials for the *n*-doping processes for **P1**−**P4** were determined to be about −1.68, −1.73, −1.77, and −1.47 V, respectively. From the onset potentials of the oxidation and reduction processes, the band gaps (E_g) of **P1**−**P4** were estimated to be about 2.20, 2.18, 2.13, and 1.81 eV, respectively.[42] These E_g values are close to those obtained from the optical absorption measurements from the film spectra (Figure 2) (vide supra). The LUMO and HOMO energy levels of **P1**−**P4** were also estimated to be −2.97, −2.92, −2.88, and −3.18 eV and −5.17, −5.10, −5.01, and −4.99 eV, respectively.

To obtain further information about the electronic structure of the copolymers, we performed DFT calculations for the basic structure units (Figure 4): **A** (for polymer **P1**), **B** (for polymers **P2** and **P3**), and **C** (for polymer **P4**). The resultant optimized geometries for **A**−**C**, along with their electrostatic potentials (ESP) and frontier molecular orbitals, are shown in Figure 4. Although the HOMO is delocalized to some extent over the π-conjugation systems, the LUMO is highly localized to the 2-pyran-4-ylidene-malononitrile (PYM) moiety. This suggests that the transition is accompanied by charge transfer (CT) from the phenyl or thiophene units to the PYM unit. Obviously, the increase in the content of thiophene units (shown in structures **B** and **C**) could enhance the CT formation. The HOMO/LUMO energy levels for **A**−**C** were calculated to be −5.10/−3.26, −4.56/−3.25, and −4.86/−3.25 eV, respectively. Thus, the calculated HOMO−LUMO energy band gap is 1.84 eV for **A**, 1.31 eV for **B**, and 1.61 eV for **C**. It was also noticed that with an increase in the number of thiophene units, the HOMO energy level increased significantly, whereas the LUMO energy level remained relatively unchanged due to its highly localized state around the PYM unit. In addition, the calculated molecular surface showed a continuous positive ESP (blue in Figure 4) along the conjugated backbone, indicating that charge carriers can migrate through this open channel. However, some negative ESP regions (yellow in Figure 4) associated with the electron-acceptor groups could facilitate the separation and transport of charge carriers generated during the photovoltaic cell operation.

3.4. Photovoltaic Properties. PVCs were fabricated with the structure of ITO/ PEDOT/PSS (30 nm)/active layer (70 nm)/ Ca (8 nm)/Al (140 nm). A blend film of the copolymer and PCBM with a weight ratio of 1:1 formed the active layer. Current−voltage (I−V) curves of the PV devices based on **P1**−**P4** are shown in Figure 5 with their photovoltaic performance parameters listed next to the corresponding I−V curves. The open-circuit voltage (V_{oc}), short-circuit current (J_{sc}), fill factor (FF), and power conversion efficiency (PCE) values of these devices under the illumination of AM1.5 (100 mW/cm^2) were measured to be 0.93 V, 0.27 mA cm^{-2}, 0.30, and 0.08% for the polymer **P1**; 0.75 V, 0.98 mA cm^{-2}, 0.29, and 0.20% for the polymer **P2**; 0.59 V, 3.80 mA cm^{-2}, 0.26, and 0.60% for the polymer **P3**; and 0.60 V, 5.03 mA cm^{-2}, 0.29, and 0.90% for the polymer **P4**, respectively. The observed increase in V_{oc} with decreasing the thiophene content from **P3** through **P2** to **P1** can be attributed to the decrease in the HOMO energy levels

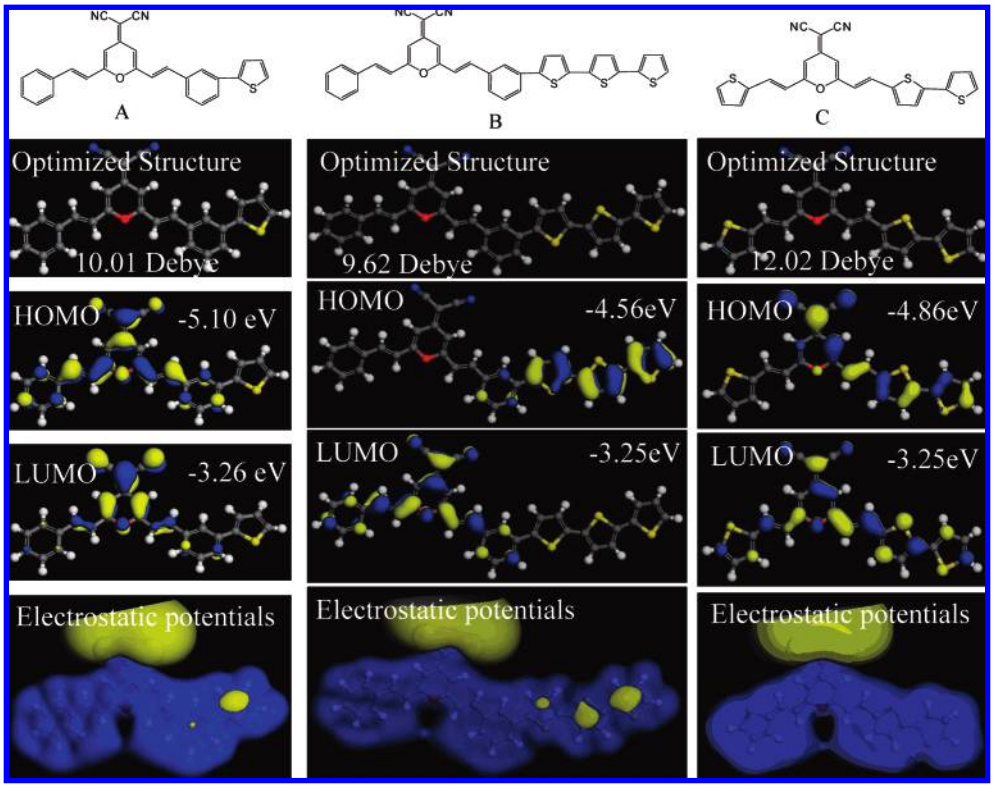

Figure 4. Calculated HOMO, LUMO, and molecular electrostatic potential (ESP) surfaces for the optimized geometries **A**−**C**.

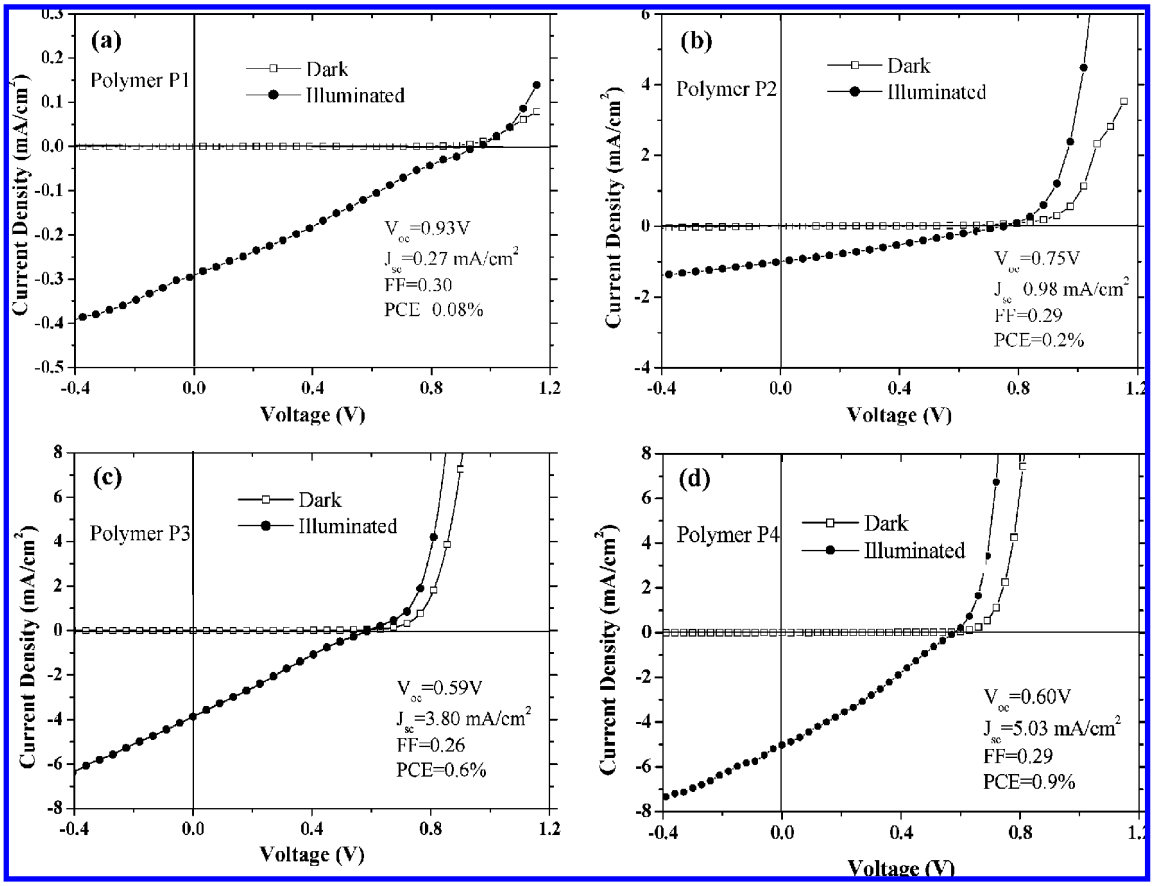

Figure 5. Current−voltage curves for photovoltaic cells based on **P1** (a), **P2** (b), **P3** (c), and **P4** (d) under AM 1.5 (100 mW/cm^2).

of the copolymers as V_{oc} depends on the energy difference between the LUMO of the acceptor (PCBM) and the HOMO of the donor (conjugated polymer).[43] Therefore, increasing the content of the acceptor unit and/or reducing the donor content increased the V_{oc} of the bulk heterojunction PVCs.[31,32] It was also noticed that J_{sc} increased from **P1** through **P2** to **P3**.

As can be seen in Figure 4 and Scheme 1, PYM and the thiophene units are connected via the meta position of the

benzene ring in the phenylene vinyl unit. Such a connection could not only disrupt the conjugation length along the polymer backbone to yield a relatively low carrier mobility but also decrease the optical absorption. Consequently, relatively low values of the PCE were observed in the present study for these PVCs based on **P1**−**P3**. When the phenyl unit in PYM was replaced by thiophene, however, the polymer **P4** showed an enhanced absorption and PCE (about 0.90%). The corresponding low FF values suggested that there is still considerable room for future improvement in the device performance through optimization of the device structure.

4. Conclusion

A class of new conjugated copolymers containing donor (thiophene)−acceptor (PYM) segments has been successfully synthesized via Stille coupling polymerization. Their molecular structures were confirmed by ^{1}HNMR and element analysis. UV−vis spectra indicated that increasing the number of thiophene units led to a red-shift in the optical absorption and strengthened the interaction of the polymer chains, and hence, there was an enhanced carrier mobility for photovoltaic applications. The band gaps calculated based on UV−vis spectra, CV scanning, and DFT modeling all indicated a narrowing band gap with increasing the donor content in the polymer structure. The LUMO and HOMO energy levels determined by the electrochemical measurements and DFT calculation also indicated that increasing the content of the donor unit increased the HOMO energy level, while the LUMO energy level remained relatively unchanged.

PVCs with the structure ITO/PEDOT/PSS (30 nm)/copolymer−PCBM blend (70 nm)/Ca (8 nm)/Al (140 nm) also were fabricated and characterized. It was demonstrated that the V_{oc} increased effectively with a decrease in the donor content in the polymer structure. Although the PC efficiencies for these unoptimized photovoltaic cells are still not sufficiently high, this study provides a novel concept for tuning the V_{oc} of bulk heterojunction photovoltaic devices by adjusting the donor/acceptor ratio within a donor-π-acceptor conjugated polymer active layer.

Acknowledgment. Financial support of this work from the Air Force Office of Scientific Research (FA9550-06-1-0384) is gratefully acknowledged.

References and Notes

(1) Sun, S.; Sacriciftci, N. S. *Organic Photovoltaics*; CRC Press: Boca Raton, FL, 2005.

(2) Sacriciftci, N. S.; Smilowitz, L.; Heeger, A. J.; Wudl, F. *Science (Washington, DC, U.S.)* **1992**, *258*, 1474.

(3) Huynh, W. U.; Dittmer, J. J.; Alivisatos, A. P. *Science (Washington, DC, U.S.)* **2002**, *295*, 2425.

(4) Kim, J. Y.; Kim, S. H.; Lee, H. H.; Lee, K.; Ma, W.; Gong, X.; Heeger, A. J. *Adv. Mater.* **2006**, *18*, 572.

(5) Shao, Y.; Yang, Y. *Adv. Mater.* **2005**, *17*, 2841.

(6) Li, G.; Shrotriya, V.; Huang, J.; Yao, Y.; Moriarty, T.; Emery, K.; Yang, Y. *Nat. Mater.* **2005**, *4*, 864.

(7) Kim, Y.; Cook, S.; Tuladhar, M.; Choulis, S. A.; Nelson, J.; Durrant, J. R.; Bradley, D. D. C.; Giles, M.; McCulloch, I.; Ha, C. S.; Ree, M. *Nat. Mater.* **2006**, *5*, 197.

(8) Hou, J. H.; Tan, Z. A.; Yan, Y.; He, Y. J.; Yang, C. H.; Li, Y. F. *J. Am. Chem. Soc.* **2006**, *128*, 4911.

(9) Shi, C. J.; Yao, Y.; Yang, Y.; Pei, Q. B. *J. Am. Chem. Soc.* **2006**, *128*, 8980.

(10) Schilinsky, P.; Waldauf, C.; Brabec, C. J. *Appl. Phys. Lett.* **2002**, *81*, 3885.

(11) Padinger, F.; Rittberger, R. S.; Sariciftci, N. S. *Adv. Funct. Mater.* **2003**, *13*, 1.

(12) Al-Ibrahim, M.; Ambacher, O.; Sensfuss, S.; Gobsch, G. *Appl. Phys. Lett.* **2005**, *86*, 201120.

(13) Reyes-Reyes, M.; Kim, K.; Carrolla, D. L. *Appl. Phys. Lett.* **2005**, *87*, 83506.

(14) Ma, W.; Yang, C.; Gong, X.; Lee, K.; Heeger, A. J. *Adv. Funct. Mater.* **2005**, *15*, 1617.

(15) Sirringhaus, H.; Brown, P. J.; Friend, R. H.; Nielsen, M. M.; Bechgaard, K.; Langeveld-Voss, B. M. W.; Spiering, A. J. H.; Janssen, R. A. J.; Meijer, E. W.; Herwig, P.; de Leeuw, D. M. *Nature (London, U.K.)* **1999**, *401*, 685.

(16) Benincori, T.; Brenna, E.; Sannicolo, F.; Trimarco, L.; Zotti, G.; Sozzani, P. *Angew. Chem., Int. Ed.* **1996**, *35*, 648.

(17) Nierengarten, J. F.; Ecker, J. F.; Nicoud, J. F.; Ouali, L.; Krasnikov, V.; Hadziioannou, G. *Chem. Commun. (Cambridge, U.K.)* **1999**, 617.

(18) Cravino, A.; Sariciftci, N. S. *J. Mater. Chem.* **2002**, *12*, 1931.

(19) Scharber, M. C.; Mühlbacher, D.; Koppe, M.; Denk, P.; Waldauf, C.; Heeger, A. J.; Brabec, C. J. *Adv. Mater.* **2006**, *18*, 789.

(20) Savenije, T. J.; Kroeze, J. E.; Yang, X. N.; Loos, J. *Adv. Funct. Mater.* **2005**, *15*, 1260.

(21) Sivula, K.; Ball, Z. T.; Watanabe, N.; Fréchet, J. M. *Adv. Mater.* **2006**, *18*, 206.

(22) Marcos Ramos, A.; Rispens, M. T.; Van Duren, J. K. J.; Hummelen, J. C.; Janssen, R. A. J. *J. Am. Chem. Soc.* **2001**, *123*, 6714.

(23) Zhang, F.; Svensson, M.; Andersson, M. R.; Maggini, M.; Bucella, S.; Menna, E.; Inganas, O. *Adv. Mater.* **2001**, *13*, 1871.

(24) Xiao, S. Q.; Wang, S.; Fang, H. J.; Li, Y. L.; Shi, Z. Q.; Du, C. M.; Zhu, D. B. *Macromol. Rapid Commun.* **2001**, *22*, 1313.

(25) Yang, C. H.; Li, H. M.; Sun, Q. J.; Qiao, J.; Li, Y. L.; Li, Y. F.; Zhu, D. B. *Sol. Energy Mater. Sol. Cells* **2005**, *85*, 241.

(26) Alam, M. M.; Jenekhe, S. A. *Chem. Mater.* **2004**, *16*, 4647.

(27) Semenikhin, O. A.; Hossain, M. M. D.; Workentin, M. S. *J. Phys. Chem. B* **2006**, *110*, 20189.

(28) Sun, S. S.; Zhang, C.; Ledbetter, A.; Choi, S.; Seo, K.; Bonner, C. E.; Drees, M.; Sariciftci, N. S. *Appl. Phys. Lett.* **2007**, *90*, 43117.

(29) Zhang, C.; Choi, S.; Haliburton, J.; Cleveland, T.; Li, R.; Sun, S. S.; Ledbetter, A.; Bonner, C. E. *Macromolecules* **2006**, *39*, 4317.

(30) Greenham, N. C.; Moratti, S. C.; Bradley, D. D. C.; Friend, R. H.; Holmes, A. B. *Nature (London, U.K.)* **1993**, *365*, 628.

(31) Shaheen, S. E.; Brabec, C. J.; Sariciftci, N. S.; Padinger, F.; Fromherz, T.; Hummelen, J. C. *Appl. Phys. Lett.* **2001**, *78*, 841.

(32) Svensson, M.; Zhang, F.; Veenstra, S. C.; Verhees, W. J. H.; Hummelen, J. C.; Kroon, J. M.; Inganäs, O.; Andersson, M. R. *Adv. Mater.* **2003**, *15*, 988.

(33) Becke, A. D. *J. Chem. Phys.* **1988**, *88*, 2547.

(34) Lee, C.; Yang, W.; Parr, R. G. *Phys. Rev. B: Condens. Matter Mater. Phys.* **1988**, *37*, 786.

(35) Yang, S. J.; Olishevski, P.; Kertesz, M. *Synth. Met.* **2004**, *141*, 171.

(36) Peng, Q.; Lu, Z. Y.; Huang, Y.; Xie, M. G.; Han, S. H.; Peng, J. B.; Cao, Y. *Macromolecules* **2004**, *37*, 260.

(37) Peng, Q.; Kang, E. T.; Neoh, K. G.; Xiao, D.; Zou, D. C. *J. Mater. Chem.* **2006**, *16*, 376.

(38) Bao, Z.; Chan, W. K.; Yu, L. *J. Am. Chem. Soc.* **1995**, *117*, 12426.

(39) Jayakannan, M.; van Dongen, L. L. J.; Janssen, R. A. J. *Macromolecules* **2001**, *34*, 5386.

(40) Dhanabalan, A.; van Dongen, J. L. J.; van Duren, J. K. J.; Janssen, H. M.; van Hal, P. A.; Janssen, R. A. J. *Macromolecules* **2001**, *34*, 2495.

(41) Yamamoto, T.; Komarudin, D.; Arai, M.; Lee, B. L.; Suganuma, H.; Asakawa, N.; Inoue, Y.; Kubota, K.; Sasaki, S.; Fukuda, T.; Matsuda, H. *J. Am. Chem. Soc.* **1998**, *120*, 2047.

(42) Mammo, W.; Admassie, S.; Gadisa, A.; Zhang, F. L.; Inganas, O.; Andersson, M. R. *Sol. Energy Mater. Sol. Cells* **2007**, *91*, 1010. Note that the HOMO and LUMO levels are calculated according to the equations HOMO = $-(E_{ox}' + 4.65)$ (eV) and LUMO = $-(E_{red}' + 4.65)$ (eV), respectively, by assuming that the energy level of Fc/Fc$^+$ is −4.8 eV below the vacuum level, where E_{ox}' and E_{red}' are the onset potentials for the first oxidation and reduction, respectively.

(43) Mihailetchi, V. D.; Blorn, P. W. M.; Hummelen, J. C.; Rispens, M. T. *J. Appl. Phys.* **2003**, *9*, 6849.